


Precision measurement of the branching fraction of $J/\psi \rightarrow K^+ K^-$ via $\psi(2S) \rightarrow \pi^+ \pi^- J/\psi$

M. Ablikim *et al.**
(BESIII Collaboration)

 (Received 22 May 2024; accepted 27 June 2024; published 8 August 2024)

Using a sample of 448.1×10^6 $\psi(2S)$ events collected with the BESIII detector, we perform a study of the decay $J/\psi \rightarrow K^+ K^-$ via $\psi(2S) \rightarrow \pi^+ \pi^- J/\psi$. The branching fraction of $J/\psi \rightarrow K^+ K^-$ is determined to be $\mathcal{B}_{K^+ K^-} = (3.072 \pm 0.023(\text{stat}) \pm 0.050(\text{syst})) \times 10^{-4}$, which is consistent with previous measurements but with significantly improved precision.

DOI: [10.1103/PhysRevD.110.032006](https://doi.org/10.1103/PhysRevD.110.032006)

I. INTRODUCTION

The decay of narrow vector states of charmonium, like J/ψ , into states of light quarks can proceed via $c\bar{c}$ annihilation into a virtual photon or three gluons. In the case of the decay to two kaons, regardless of the charge of the kaons, both strong and electromagnetic interactions contribute with comparable strength, and the branching fraction (BF) depends critically on their relative phase [1]. Neglecting the interference between the continuum and resonance amplitudes may affect the measurement of the BF, $\mathcal{B}_{K^+ K^-}$, in the reaction $e^+ e^- \rightarrow K^+ K^-$.

Early phenomenological studies argued that this relative phase is quite large, close to $\pm 90^\circ$ [2–5]. The contribution of the continuum has been investigated also in Refs. [6,7], showing that the interference between continuum and resonance amplitudes may affect the J/ψ decays. Furthermore, the authors show the crucial role in confirming the large universal phase between the strong and the electromagnetic amplitudes, which can affect precision measurements of the branching ratio of charmonia decays with special focus on the decays in two pseudoscalars. In Ref. [1], it is demonstrated that the direct coupling of J/ψ to the hadronic final state is important in the $K^+ K^-$ case and a combination of measurements on and off resonance is essential to obtain the relative magnitude and phase of quantum electrodynamics (QED) and hadronic amplitudes.

The most recent $\mathcal{B}_{K^+ K^-}$ measurement was reported by BABAR [8], using the untagged initial state radiation (ISR) technique, to be $\mathcal{B}_{K^+ K^-} = (3.36 \pm 0.20(\text{stat}) \pm 0.12(\text{syst})) \times 10^{-4}$. They applied a correction for the effect

of the interference with the continuum, after the determination of the relative phase, by combining their result and the ones from other experiments for the $J/\psi \rightarrow K_S^0 K_L^0$ decay [9,10]. By using the result from Ref. [9], the BABAR collaboration determined a relative phase $\varphi = (97 \pm 5)^\circ$ or $(-97 \pm 5)^\circ$; on the other hand, by using the results in Ref. [10], the phase was determined to be $\varphi = (111 \pm 5)^\circ$ or $(-109 \pm 5)^\circ$. Using the latter determination of φ , $\mathcal{B}_{K^+ K^-}$ was measured to be $(3.22 \pm 0.20(\text{stat}) \pm 0.12(\text{syst})) \times 10^{-4}$ or $(3.50 \pm 0.20(\text{stat}) \pm 0.12(\text{syst})) \times 10^{-4}$, depending on the sign of the phase. It is worthwhile to notice that the shifts due to the interference are large, i.e., about 5%, and should be taken into account in the $e^+ e^- \rightarrow K^+ K^-$ reaction for precision measurements.

The study of this decay channel, by means of $\psi(2S) \rightarrow \pi^+ \pi^- J/\psi$, allows us to measure $\mathcal{B}_{K^+ K^-}$ with no need to take into account the interference of the resonant amplitude with the continuum. It is advantageous, being the most probable $\psi(2S)$ decay ($\mathcal{B}(\psi(2S) \rightarrow \pi^+ \pi^- J/\psi) = (34.98 \pm 0.02 \pm 0.45)\%$ [11]), and the most accessible experimentally. For studies of J/ψ decays, the J/ψ events can be tagged by the recoiling mass against the $\pi^+ \pi^-$ system in the decay $\psi(2S) \rightarrow \pi^+ \pi^- J/\psi$. This J/ψ sample is automatically free of any contamination of $K^+ K^-$, $p\bar{p}$, $\mu^+ \mu^-$ and $e^+ e^-$ produced directly at the center of mass energy (cme) of $\sqrt{s} = 3.097$ GeV. The continuum contribution is negligible in the subsequent J/ψ decay, making this sample relatively clean and simple to analyze. The most recent measurement of $\mathcal{B}_{K^+ K^-}$ in this channel was performed by Metreveli *et al.* using CLEO-c data [10], with a result of $(2.86 \pm 0.09 \pm 0.19) \times 10^{-4}$; this measurement currently is the only one determining the world average by the Particle Data Group (PDG) [12]. In the same article the relative phase in J/ψ decays into pseudoscalar pairs was reported to be $\varphi = (73.5_{-4.5}^{+5.0})^\circ$, obtained by means of the BFs of $J/\psi \rightarrow K^+ K^-$, $J/\psi \rightarrow \pi^+ \pi^-$ and $J/\psi \rightarrow K_S^0 K_L^0$.

*Full author list given at the end of the article.

Published by the American Physical Society under the terms of the [Creative Commons Attribution 4.0 International license](https://creativecommons.org/licenses/by/4.0/). Further distribution of this work must maintain attribution to the author(s) and the published article's title, journal citation, and DOI. Funded by SCOAP³.

A sample of 448.1×10^6 $\psi(2S)$ events collected in 2009 and 2012 with the BESIII detector offers, by virtue of being about 20 times larger than the CLEO-c statistics, a unique opportunity to improve the precision of $\mathcal{B}_{K^+K^-}$. It is worthwhile to notice that the sign of $\sin\varphi$ for J/ψ decays can be determined experimentally from the relative difference, $\delta\mathcal{B}_{K^+K^-}/\mathcal{B}_{K^+K^-}$, between precise measurements of BFs in both $e^+e^- \rightarrow K^+K^-$ reaction and $\psi(2S) \rightarrow \pi^+\pi^-J/\psi$, as suggested in Ref. [8].

This paper describes the measurement of $\mathcal{B}_{K^+K^-}$ via $\psi(2S) \rightarrow \pi^+\pi^-J/\psi$ with BESIII data and it is organized as follows. Section II contains a brief description of the BESIII detector and data and Monte Carlo (MC) samples. In Sec. III we describe the analysis strategy, that foresees a measurement relative to the precisely measured BF of the $J/\psi \rightarrow \mu^+\mu^-$ decay. In Sec. IV we present the event selection and in Sec. V the background evaluation can be found. The $\mathcal{B}_{K^+K^-}$ measurement is presented in Sec. VI while the systematic uncertainties are discussed in Sec. VII. Sec. VIII, with summary and conclusions, closes the paper.

II. BESIII DETECTOR, DATA AND MC SAMPLES

In this analysis we use two large data samples of $\psi(2S)$ decays, collected with the BESIII detector in 2009 and in 2012. The numbers of $\psi(2S)$ events were determined to be $(107.0 \pm 0.8) \times 10^6$ and $(341.1 \pm 2.1) \times 10^6$ [13], respectively. The BESIII detector records symmetric e^+e^- collisions provided by the BEPCII storage ring [14], which operates in the cme range from 2.00 to 4.95 GeV. BESIII has collected large data samples in this energy region [15]. The cylindrical core of the BESIII detector covers 93% of the full solid angle and consists of a helium-based multilayer drift chamber (MDC), a plastic scintillator time-of-flight system (TOF), and a CsI(Tl) electromagnetic calorimeter (EMC), which are all enclosed in a superconducting solenoidal magnet providing a 1.0 T (0.9 T in 2012) magnetic field. The solenoid is supported by an octagonal flux-return yoke with resistive plate counter muon identification modules interleaved with steel.

The charged-particle momentum resolution at 1 GeV/ c is 0.5%, and the resolution of the specific energy loss, dE/dx , is 6% for electrons from Bhabha scattering. The EMC measures photon energies with a resolution of 2.5% (5%) at 1 GeV in the barrel (end cap) region. The time resolution in the TOF barrel region is 68 ps, while that in the end cap region is 110 ps. Details about the design and performance of the BESIII detector are given in Ref. [16].

Monte Carlo simulated data samples produced with a GEANT4-based [17] software package, which includes the geometric description of the BESIII detector [18] and the detector response, are used to determine detection efficiencies, to estimate backgrounds and for event selection optimization. The simulation models the beam energy spread and ISR in the e^+e^- annihilations with the generator

KKMC [19,20]. An inclusive MC (INC-MC) sample includes the production of the $\psi(2S)$ resonance, the ISR production of J/ψ , and the continuum processes incorporated in KKMC [19–21]. All particle decays are modeled with EVTGEN [21,22] using BFs either taken from the PDG [23], when available, or otherwise estimated with LUNDCHARM [24,25]. Final state radiation (FSR) from charged final state particles is incorporated using the PHOTOS package [26]. The INC-MC samples correspond to 106 millions $\psi(2S)$ events for 2009 and 400 millions $\psi(2S)$ events for 2012.

To evaluate the detection efficiency, exclusive signal MC simulations are performed with equivalent sizes much larger than the expected data statistics. The $\psi(2S)$ production has been previously described and the subsequent decays are generated using EVTGEN [21,22] with the JPIPI module for $\psi(2S) \rightarrow \pi^+\pi^-J/\psi$, VSS for $J/\psi \rightarrow K^+K^-$ and VLL for $J/\psi \rightarrow \mu^+\mu^-$.

III. METHOD

In order to reduce the experimental systematic uncertainties, the BF of $J/\psi \rightarrow K^+K^-$ is determined relative to the well known $J/\psi \rightarrow \mu^+\mu^-$ channel. The strategy for this analysis is to measure the ratio

$$\mathcal{R} \equiv \frac{\mathcal{B}_{K^+K^-}}{\mathcal{B}_{\mu^+\mu^-}}. \quad (1)$$

This ratio can be rewritten as

$$\mathcal{R} = \frac{\mathcal{B}_{K^+K^-}}{\mathcal{B}_{\mu^+\mu^-}} = \frac{N_{K^+K^-} \times \epsilon_{\mu^+\mu^-}}{N_{\mu^+\mu^-} \times \epsilon_{K^+K^-}}, \quad (2)$$

where $N_{K^+K^-}$ and $N_{\mu^+\mu^-}$ are the observed numbers of events of $J/\psi \rightarrow K^+K^-$ and $J/\psi \rightarrow \mu^+\mu^-$, respectively, while $\epsilon_{K^+K^-}$ and $\epsilon_{\mu^+\mu^-}$ are the corresponding reconstruction efficiencies. In this way, the systematic uncertainties in the total number of $\psi(2S)$ events and the tracking efficiencies of charged particles, are canceled in the \mathcal{R} measurement. Combining the obtained \mathcal{R} with the precise world average of $\mathcal{B}_{\mu^+\mu^-}$ from the PDG [23], $(5.916 \pm 0.033)\%$, $\mathcal{B}_{K^+K^-}$ can be measured.

IV. EVENT SELECTION

The channel we are investigating is $\psi(2S) \rightarrow \pi^+\pi^-J/\psi$ with the subsequent decay $J/\psi \rightarrow K^+K^-$.

The total number of charged tracks in an event must be four with net charge equal to zero. Charged tracks are reconstructed using the MDC. For each track, the point of closest approach to the interaction point must be within 1 cm in the plane perpendicular to the beam direction and within 10 cm along the beam direction. Moreover, to guarantee better agreement between data and MC simulation, we require them to have a polar angle in the range

$-0.80 < \cos \theta < 0.80$, where θ is defined with respect to the z -axis, taken to be the symmetry axis of the MDC. Furthermore, a vertex fit in which all charged tracks are forced to originate from a common vertex is performed and required to be successful. The parameters of daughter tracks after the vertex fit are updated.

We require two pion candidates and two kaon candidates, both oppositely charged, in each event. No particle identification is required to avoid additional systematic uncertainty. The two tracks with lower momentum (less than $1.0 \text{ GeV}/c$) are assigned as the pion candidates, as expected by the exclusive MC sample. To veto the background events associated with photon conversion we require the cosine of the opening angle between the two pions, $\cos \theta_{\pi\pi}$, to be less than 0.5. The recoiling mass against the two selected pions is calculated as

$$\text{RM}(\pi^+\pi^-) = \sqrt{(p_{\text{cme}} - p_{\pi^+} - p_{\pi^-})^2} \quad (3)$$

where p_{cme} and p_{π^\pm} are the four-momenta in the center of mass system and for the two charged pion candidates, respectively. The recoiling mass $[\text{RM}(\pi^+\pi^-)]$ distribution of the accepted candidates is shown in Fig. 1, dominated by the production of the J/ψ resonance. To tag the J/ψ production, the $\text{RM}(\pi^+\pi^-)$ range between 3.087 and $3.107 \text{ GeV}/c^2$ is required, corresponding to about $\pm 5\sigma_v$, where the width σ_v is obtained by fitting the $\text{RM}(\pi^+\pi^-)$ distribution with a Voigt function. The remaining two good charged particles can be kaon candidates, for which we require their momenta greater than $1.2 \text{ GeV}/c$, as suggested by the exclusive signal MC sample. The opening angle $\theta_{K^+K^-}$ between the two decay products is calculated in the reference frame of the J/ψ , requiring $\cos \theta_{K^+K^-} < -0.95$. The yields of the $J/\psi \rightarrow e^+e^-$ and $J/\psi \rightarrow \mu^+\mu^-$ overwhelm the $J/\psi \rightarrow K^+K^-$ one, since their BFs are several orders of magnitude larger. To veto the background

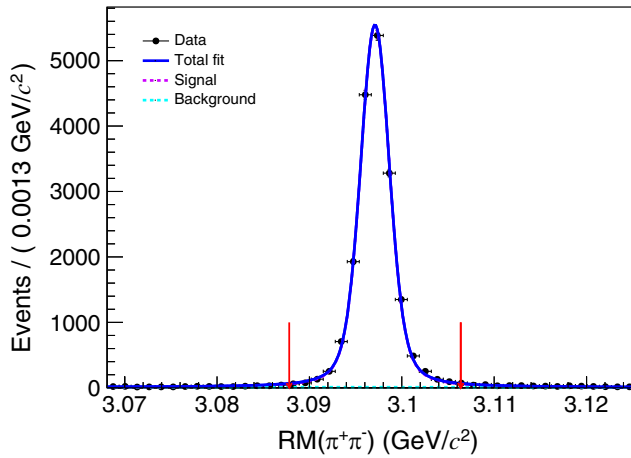


FIG. 1. Distribution of $\text{RM}(\pi^+\pi^-)$ against the $(\pi^+\pi^-)$ system of the selected candidates. The best fit of a Voigt function to the data is shown as the blue line. The red arrows show the $\pm 5\sigma_v$ range.

of $J/\psi \rightarrow e^+e^-$, an efficient selection can be found using the ratio E_{dep}/p , in which E_{dep} is the energy deposited in the EMC and p is the reconstructed momentum in the MDC for a decay product of J/ψ , requiring it to be less than $0.8c$. Further selection is applied on the total energy deposited in the EMC for an event, E_{EMC} , which is required to be between 0.3 and 2.5 GeV . To perform the measurement of $\mathcal{B}_{K^+K^-}$, we calculate the scaled visible energy (X_{vis}) of the two particles in the decay final state, which are K^+ and K^- candidates, as

$$X_{\text{vis}} = \frac{E_{K^+} + E_{K^-}}{E_{J/\psi}}, \quad (4)$$

where E_{K^\pm} are the energies of the kaon candidates calculated using the kaon mass hypothesis in the center-of-mass frame and $E_{J/\psi}$ is the J/ψ energy, in the same reference frame, corresponding to the J/ψ rest mass. The $J/\psi \rightarrow K^+K^-$ signal is expected to center around $X_{\text{vis}} = 1.0$, while at lower values two final state particles with higher mass can be found, mainly from $J/\psi \rightarrow p\bar{p}$ decay due to the lack of PID requirements, and at higher values the ones with lower mass (mainly $J/\psi \rightarrow \mu^+\mu^-$). We define two different intervals in X_{vis} to tag the two decays of interest: the $J/\psi \rightarrow K^+K^-$ signal region (KK signal region) and the $J/\psi \rightarrow \mu^+\mu^-$ signal region (dimuon region), between 0.98 and 1.01 and between 1.02 and 1.07 , respectively. The asymmetric range of the KK signal region is chosen because of the significant tail of the $J/\psi \rightarrow \mu^+\mu^-$ distribution, shown in Fig. 2, where the MC distributions are shown for INC-MC with MC-truth

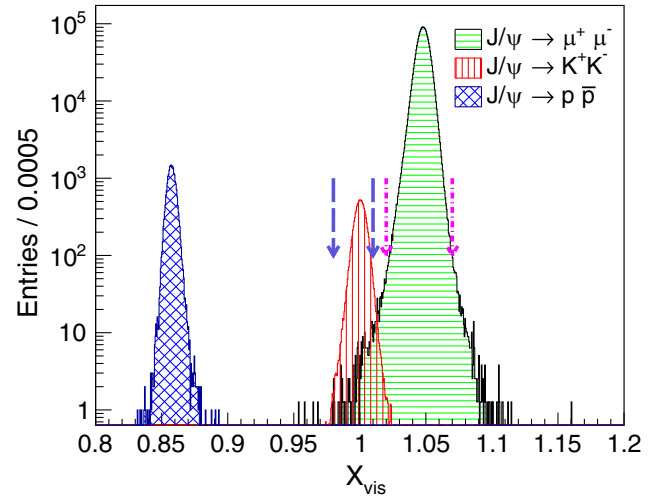


FIG. 2. Distribution of X_{vis} , for the INC-MC sample, with MC-truth matching applied, in log-scale, pattern-filled with vertical lines in red for $J/\psi \rightarrow K^+K^-$, with horizontal lines in green for $J/\psi \rightarrow \mu^+\mu^-$ and with oblique squares in blue for $J/\psi \rightarrow p\bar{p}$. The purple dashed line arrows show the KK signal region and the magenta dot dashed line ones the dimuon region, as described in the text.

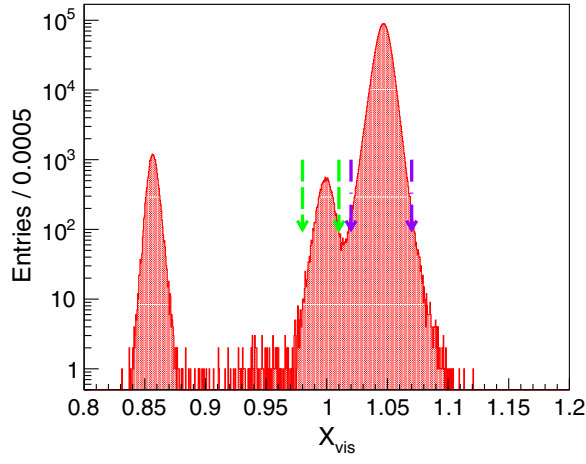


FIG. 3. Distribution of X_{vis} for data, in log-scale. The green dashed line arrows show the KK signal region and the purple dot dashed line ones the dimuon region, as described in the text.

matching for the $J/\psi \rightarrow K^+K^-$ and $J/\psi \rightarrow \mu^+\mu^-$ decays. Momentum conservation in the reconstructed J/ψ decays is required by demanding, in the decay, the magnitude of the normalized vector sum of the total momentum, $|\sum_i \mathbf{p}_i|/E_{J/\psi}$, to be less than 0.025. This allows us to reject most of the background from decays to more than two bodies.

After all these requirements the X_{vis} distribution features three structures, as shown in Fig. 3. The one centering around $X_{\text{vis}} = 0.85$ is well separated, and consists mainly of the residual $J/\psi \rightarrow p\bar{p}$ decays. A further selection is applied, requiring the X_{vis} to be greater than 0.90. The third structure, centering around $X_{\text{vis}} = 1.05$, is well separated, but the tail in the KK signal region must be evaluated in the fit procedure.

V. BACKGROUND ESTIMATION

We perform a background study using the INC-MC samples, described in Sec. II, thanks to the MC-truth matching and to the TopoAna package [27]. After all the selections, except the X_{vis} ones, described in Sec. IV, the main background components are shown in Fig. 4. In the dimuon region, the background is mainly due to $\psi(2S) \rightarrow \pi^+\pi^-J/\psi, J/\psi \rightarrow e^+e^-/\pi^+\pi^-$ (B1/B2), accounting for about 0.67%, as shown in the bottom of Fig. 4. Non- $\pi^+\pi^-J/\psi$ background is negligible. In KK signal region, the background fraction is about 6%. It is dominated by non- $\pi^+\pi^-J/\psi$ events that account for about 70% of the total background, while about 30% is due to the tail of $J/\psi \rightarrow \mu^+\mu^-$, dominating the background involving J/ψ production as shown in Fig. 4. This background can be subtracted in the fit procedure. The non- $\pi^+\pi^-J/\psi$ background is a peaking background, mainly involving the $K_1(1270)^\pm$ resonance production. The main background channel (charge conjugation is implied) is the decay

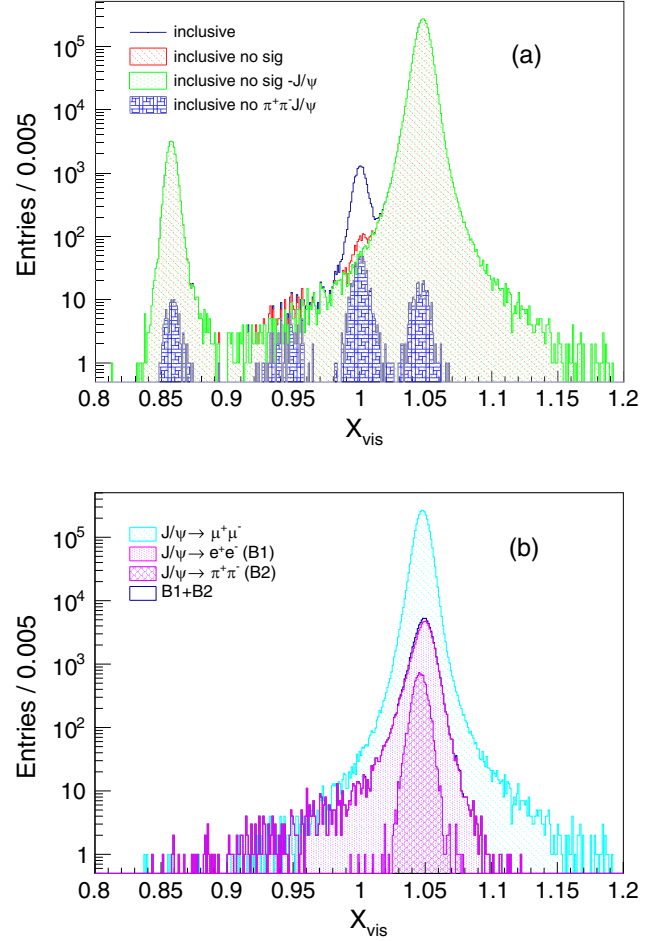


FIG. 4. Distributions of X_{vis} for the inclusive Monte Carlo sample, broken down according to MC truth information. In the figure (a), the X_{vis} distribution for events in KK signal region is plotted. The blue line indicates the total INC-MC distribution, the red histogram gives all background events in KK signal region, and the green and blue histograms give background events with a J/ψ and without $\pi^+\pi^-J/\psi$, respectively. Likewise, the plot (b) shows the X_{vis} distribution for dimuon region broken down into its relevant contributions B1 and B2, as described in the text.

$\psi(2S) \rightarrow K^-K_1(1270)^+$ with the subsequent decays $K_1(1270)^+ \rightarrow \pi^+K_0^*(1430)$ and $K_0^*(1430) \rightarrow \pi^-K^+$. Large uncertainties on the decay BF's related to these channels are reported in the PDG [12]. For this reason, the non- $\pi^+\pi^-J/\psi$ background fraction in KK signal region is evaluated by a data-driven method. An unbinned extended maximum likelihood fit is performed to the $\text{RM}(\pi^+\pi^-)$ distribution in KK signal region in the range $[3.02-3.15]$ GeV/c^2 . The signal (all J/ψ decays) is modeled by the MC-simulated signal shape, convolved with a Gaussian resolution function to account for data-MC differences, and the background by a second-order Chebyshev polynomial function. The parameters of the Gaussian and all yields are left free in the fit. The integral of the best fit function in the defined signal range,

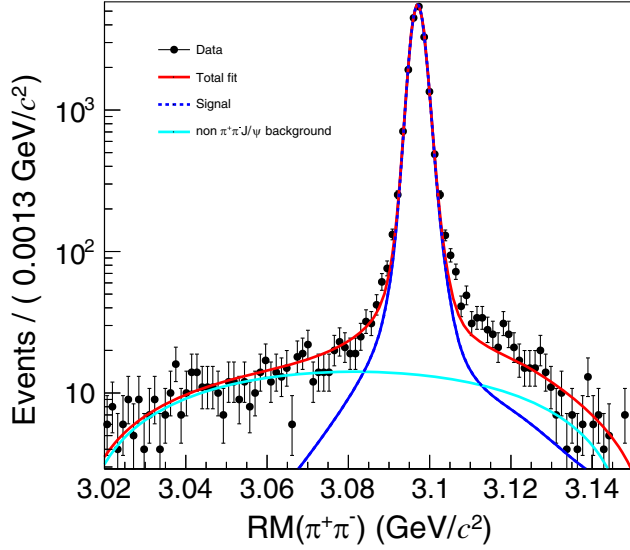


FIG. 5. Distribution of $RM(\pi^+\pi^-)$ of the accepted candidates for the full data sample with the best fit result in KK signal region in red in logarithmic scale. The signal is shown with blue dashed line and the non- $\pi^+\pi^-J/\psi$ background in cyan. The black points are data.

[3.087, 3.107] GeV/c^2 , allows us to evaluate the peaking background contribution, as shown in Fig. 5. The ratio between non- $\pi^+\pi^-J/\psi$ background and the total number of events is found to be $(1.110 \pm 0.157)\%$, $(1.257 \pm 0.095)\%$ and $(1.145 \pm 0.079)\%$ for the 2009, 2012, and 2009 + 2012 (full) data samples, respectively.

VI. MEASUREMENT OF THE BRANCHING FRACTION OF $J/\psi \rightarrow K^+K^-$

A. Signal yields and efficiencies

The yields of the J/ψ decays into two charged kaons and into two muons can be determined simultaneously by a fit to the X_{vis} distribution, as defined in Eq. (4). In the fit, the tail of $\mu^+\mu^-$ distribution in KK signal region can be evaluated and subtracted. An unbinned extended maximum likelihood fit is performed. The probability density functions are MC-simulated shapes, extracted from the exclusive MC samples and convolved with a single Gaussian function for the $J/\psi \rightarrow K^+K^-$ decay and a double-Gaussian function for the $J/\psi \rightarrow \mu^+\mu^-$ contribution. The parameters of the Gaussians and both the yields are left free in the fit. The peaking background in KK signal region is described by a Gaussian function, with the parameters fixed to the best fit ones obtained from the INC-MC sample, selected by MC-truth matching. The background fraction is fixed to the ratio determined by the data-driven method as described in Sec. V. The peaking background in dimuon region is described by a single MC-simulated shape for both $J/\psi \rightarrow e^+e^-$ and $J/\psi \rightarrow \pi^+\pi^-$ decays, extracted

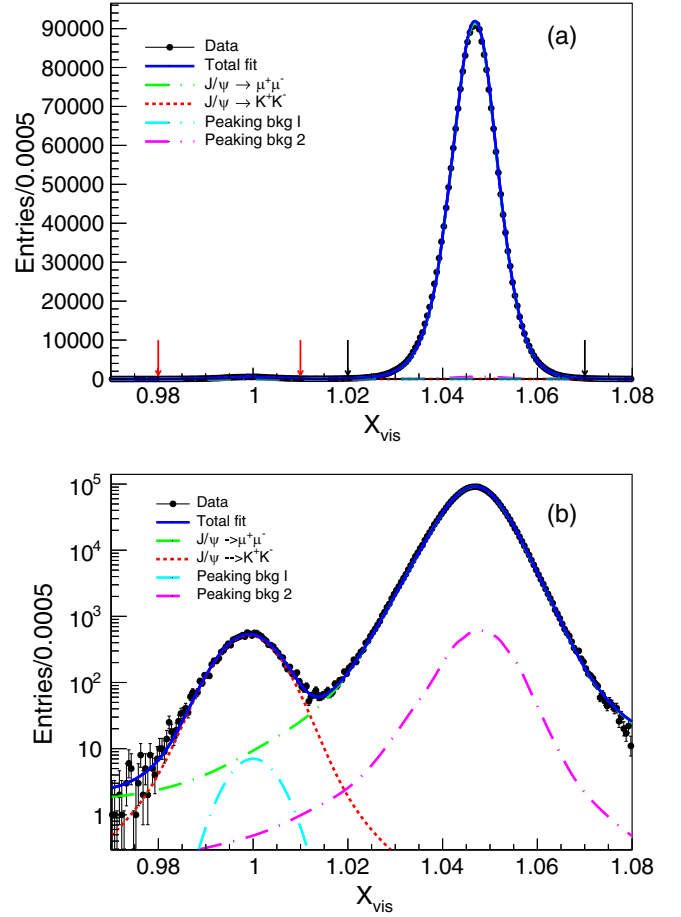


FIG. 6. Distribution of X_{vis} with the best fit results (blue line) in the full range in linear scale (a). Plot (b) shows the same distribution in logarithmic scale to better appreciate the fit results in KK signal region. The different contributions are shown by dotted curves: in red $J/\psi \rightarrow K^+K^-$, in green $J/\psi \rightarrow \mu^+\mu^-$, while in cyan and magenta the two peaking backgrounds (peaking background 1 and 2) in KK signal region (red dashed arrows) and dimuon region (black dot-dashed arrows), respectively, as described in the text. The black points are data.

from the INC-MC sample with MC-truth matching, as well. The background fraction is fixed to the INC-MC value in this case. In Fig. 6 the fit results are shown for the full data sample. The yields $N_{K^+K^-}$ and $N_{\mu^+\mu^-}$ are determined by the integral of the fit function in KK and dimuon region, respectively. An input/output check is performed by means of pseudoexperiments. We use 1000 MC samples, each with the same size of data, to check the pull distribution and no bias is found, confirming the stability of the fit procedure. The efficiencies for both $J/\psi \rightarrow K^+K^-$ and $J/\psi \rightarrow \mu^+\mu^-$ are determined by means of exclusive MC samples, described in Sec. II, separately for the two data samples. The full-sample efficiencies, determined with a weighting procedure, are $\epsilon_{\mu^+\mu^-} = 0.3269 \pm 0.0006$ and $\epsilon_{K^+K^-} = 0.3732 \pm 0.0006$.

TABLE I. The efficiencies (ϵ) and the yields (N) for both $J/\psi \rightarrow \mu^+\mu^-$ and $J/\psi \rightarrow K^+K^-$ decays, indicated in the subscript.

$\epsilon_{K^+K^-}$	0.3732 ± 0.0006
$\epsilon_{\mu^+\mu^-}$	0.3269 ± 0.0006
$N_{K^+K^-}$	$18\,176 \pm 135$
$N_{\mu^+\mu^-}$	$3\,026\,803 \pm 17\,409$

B. BF results

The ratio $\mathcal{R} = 0.005153 \pm 0.000041$ is determined from Eq. (2), using the yields and efficiencies extracted and reported in Table I. Using the PDG $\mathcal{B}_{\mu^+\mu^-}$ [23], we measure $\mathcal{B}_{K^+K^-} = (3.072 \pm 0.023) \times 10^{-4}$. The same procedure has been used for the 2012 and 2009 data samples separately with results in agreement with those of the full data sample. A further input/output check is performed using the INC-MC sample, confirming the absence of bias in the BF measurement with an agreement between the branching ratio used for generation and the determined one within 1 sigma.

VII. SYSTEMATIC UNCERTAINTIES

In the following, the contributions to the systematic uncertainties, as summarized in Table II, are discussed. In the ratio \mathcal{R} of BFs, defined in Eq. (2), the systematic uncertainties for the tracking efficiency of the charged tracks and for the number of $\psi(2S)$ cancel.

The relative uncertainty due to the finite size (750 000 events) of the exclusive MC sample used for the calculation of efficiency is calculated by binomial error calculation, resulting in 0.2%. For all the sources related to the event selection, the systematic uncertainty is calculated from the maximum difference between the $\mathcal{B}_{K^+K^-}$ values obtained by changing the selection and the nominal one, with both the efficiency and the signal yield being affected by the event selections. This selection is used to tag the J/ψ and reject the background, mostly the non- $\pi^+\pi^-J/\psi$ background. In detail the recoiling mass window is modified from about 5σ to 4σ and we calculate the difference in the $\mathcal{B}_{K^+K^-}$. The relative uncertainty is 0.30%. The limits for $\cos\theta$ is tightened to be ± 0.7 .

TABLE II. Relative systematic uncertainties in the BF measurement.

Source	Systematic uncertainty (%)
Event selection	1.5
MC statistics	0.2
Background	0.2
$\mathcal{B}_{\mu^+\mu^-}$	0.5
Total	1.6

The corresponding uncertainty is negligible, being less than 2×10^{-5} . We change the selections on $\cos\theta_{\pi\pi}$ and $\cos\theta_{KK}$ to estimate the related systematic uncertainty. In the first case we change the upper limit on $\cos\theta_{\pi\pi}$ from 0.5 to 0.6, and in the second case we change the upper limit on $\cos\theta_{K^+K^-}$ from -0.95 to -0.9 . In either case, the systematic uncertainty is negligible, being less than 5×10^{-5} . We modify the selection lowering the kaon momenta cut to 1.0 GeV/c. The uncertainty is negligible, being around 2×10^{-5} . The normalized net momentum selection is changed by ± 0.05 , keeping the largest difference in \mathcal{B} as systematic uncertainty. It is found to be 1.00%. The E_{dep}/p upper limit is changed to 0.7 and 0.9, taking the larger difference as the systematic uncertainty with a value of 0.7%. The E_{EMC} window is modified to [0.35, 2.45] and [0.25, 2.55] GeV. The systematic uncertainty is found to be 0.5%. The X_{vis} range, which defines the signal range after fitting, is changed from the chosen asymmetric window, fixed to [0.98, 1.01], due to the dimuon peak in the higher X_{vis} values range, to $[-4\sigma, +2\sigma]$, where the σ is obtained from the full width at half maximum of the signal distribution. The systematics is 0.6%. The total relative systematic uncertainty on the event selection is 1.50%. The uncertainty due to the peaking background fraction is obtained as the maximum variation in the $\mathcal{B}_{K^+K^-}$ changing the background fraction by $\pm 1\sigma$. The uncertainty is evaluated to be 0.2%. The systematic uncertainty for $\mathcal{B}_{\mu^+\mu^-}$ is quoted from the PDG as 0.5% [23]. The uncertainty due to the fit procedure is estimated by adding an additional flat background function and results in being negligible. Furthermore a study of pseudoexperiments is performed to evaluate additional systematics in the fitting procedure, and no fit bias is found. The sum in quadrature of all the contributions gives a relative total systematic uncertainty of 1.6%, corresponding to 0.050×10^{-4} .

VIII. SUMMARY

We have performed a precision measurement of the BF of the decay of $J/\psi \rightarrow K^+K^-$ to be $\mathcal{B}_{K^+K^-} = (3.072 \pm 0.023(\text{stat}) \pm 0.050(\text{syst})) \times 10^{-4}$, still dominated by the systematic uncertainty. This is an improvement by more than a factor of three over the previous measurement of $(2.86 \pm 0.21) \times 10^{-4}$ [10], obtained using the CLEO-c data, that is up to now the PDG value, with central value in agreement with that BF result. The most precise measurement of the $\mathcal{B}_{K^+K^-}$ in direct reaction, which takes into account the interference effect, is the *BABAR* one [8], in which they gave an indication of the positive sign of the relative phase. Due to their large uncertainties, our result is in agreement with both $\mathcal{B}_{K^+K^-}^{\text{BABAR}^+} = (3.22 \pm 0.20 \pm 0.12) \times 10^{-4}$ with positive phase within less than 1σ and $\mathcal{B}_{K^+K^-}^{\text{BABAR}^-} = (3.50 \pm 0.20 \pm 0.12) \times 10^{-4}$ with negative phase within about 2σ . Our result represents the first step in the path to determine the sign of the relative phase

between strong and electromagnetic amplitudes in this channel. A measurement in the $e^+e^- \rightarrow K^+K^-$ process with improved precision will complete the picture.

ACKNOWLEDGMENTS

The BESIII Collaboration thanks the staff of BEPCII and the IHEP computing center for their strong support. This work is supported in part by National Key R&D Program of China under Contracts No. 2020YFA0406300, No. 2020YFA0406400; National Natural Science Foundation of China (NSFC) under Contracts No. 11635010, No. 11735014, No. 11835012, No. 11935015, No. 11935016, No. 11935018, No. 11961141012, No. 12025502, No. 12035009, No. 12035013, No. 12061131003, No. 12192260, No. 12192261, No. 12192262, No. 12192263, No. 12192264, No. 12192265, No. 12221005, No. 12225509, No. 12235017; the Chinese Academy of Sciences (CAS) Large-Scale Scientific Facility Program; the CAS Center for Excellence in Particle Physics (CCEPP); Joint Large-Scale Scientific Facility Funds of the NSFC and CAS under Contract No. U1832207; CAS

Key Research Program of Frontier Sciences under Contracts No. QYZDJ-SSW-SLH003, No. QYZDJ-SSW-SLH040; 100 Talents Program of CAS; The Institute of Nuclear and Particle Physics (INPAC) and Shanghai Key Laboratory for Particle Physics and Cosmology; European Union's Horizon 2020 research and innovation programme under Marie Skłodowska-Curie grant agreement under Contract No. 894790; German Research Foundation DFG under Contracts Nos. 455635585, Collaborative Research Center CRC 1044, FOR5327, GRK 2149; Istituto Nazionale di Fisica Nucleare, Italy; Ministry of Development of Turkey under Contract No. DPT2006K-120470; National Research Foundation of Korea under Contract No. NRF-2022R1A2C1092335; National Science and Technology fund of Mongolia; National Science Research and Innovation Fund (NSRF) via the Program Management Unit for Human Resources & Institutional Development, Research and Innovation of Thailand under Contract No. B16F640076; Polish National Science Centre under Contract No. 2019/35/O/ST2/02907; The Swedish Research Council; U.S. Department of Energy under Contract No. DE-FG02-05ER41374.

-
- [1] H. Czyz and J. H. Kuhn, *Phys. Rev. D* **80**, 034035 (2009).
 [2] M. Suzuki, *Phys. Rev. D* **63**, 054021 (2001).
 [3] J. L. Rosner, *Phys. Rev. D* **60**, 074029 (1999).
 [4] M. Suzuki, *Phys. Rev. D* **60**, 051501(R) (1999).
 [5] G. López Castro, J. L. Lucio M., and J. Pestieau, *AIP Conf. Proc.* **342**, 441 (1995).
 [6] C. Z. Yuan, P. Wang, and X. H. Mo, *Phys. Lett. B* **567**, 73 (2003).
 [7] P. Wang, C. Z. Yuan, X. H. Mo, and D. H. Zhang, *Phys. Lett. B* **593**, 89 (2004).
 [8] J. P. Lees *et al.* (BABAR Collaboration), *Phys. Rev. D* **92**, 072008 (2015).
 [9] J. Z. Bai *et al.* (BES Collaboration), *Phys. Rev. D* **69**, 012003 (2004).
 [10] Z. Metreveli, S. Dobbs, A. Tomaradze, T. Xiao, K. K. Seth, J. Yelton, D. M. Asner, G. Tatishvili, and G. Bonvicini, *Phys. Rev. D* **85**, 092007 (2012).
 [11] M. Ablikim *et al.* (BESIII Collaboration), *Phys. Rev. D* **88**, 032007 (2013).
 [12] R. L. Workman *et al.* (Particle Data Group), *Prog. Theor. Exp. Phys.* **2022**, 083C01 (2022).
 [13] M. Ablikim *et al.* (BESIII Collaboration), *Chin. Phys. C* **42**, 023001 (2018).
 [14] C. Yu *et al.*, *Proceedings of International Particle Accelerator Conference (IPAC'16), Busan, Korea, 2016*, International Particle Accelerator Conference Vol. 1014 (JACoW, Geneva, Switzerland, 2016), 10.18429/JACoW-IPAC2016-TUYA01.
 [15] M. Ablikim *et al.* (BESIII Collaboration), *Chin. Phys. C* **44**, 040001 (2020).
 [16] M. Ablikim *et al.* (BESIII Collaboration), *Nucl. Instrum. Methods Phys. Res., Sect. A* **614**, 345 (2010).
 [17] S. Agostinelli *et al.* (GEANT4 Collaboration), *Nucl. Instrum. Methods Phys. Res., Sect. A* **506**, 250 (2003).
 [18] K.-X. Huang *et al.*, *Nucl. Sci. Tech.* **33**, 142 (2022).
 [19] S. Jadach, B. F. L. Ward, and Z. Was, *Phys. Rev. D* **63**, 113009 (2001).
 [20] S. Jadach, B. F. L. Ward, and Z. Was, *Comput. Phys. Commun.* **130**, 260 (2000).
 [21] R.-G. Ping, *Chin. Phys. C* **32**, 599 (2008).
 [22] D. J. Lange, *Nucl. Instrum. Methods Phys. Res., Sect. A* **462**, 152 (2001).
 [23] C. Patrignani *et al.* (Particle Data Group), *Chin. Phys. C* **40**, 100001 (2016).
 [24] J. C. Chen, G. S. Huang, X. R. Qi, D. H. Zhang, and Y. S. Zhu, *Phys. Rev. D* **62**, 034003 (2000).
 [25] R.-L. Yang, R.-G. Ping, and H. Chen, *Chin. Phys. Lett.* **31**, 061301 (2014).
 [26] E. Richter-Was, *Phys. Lett. B* **303**, 163 (1993).
 [27] X. Zhou, S. Du, G. Li, and C. Shen, *Comput. Phys. Commun.* **258**, 107540 (2021).
-

M. Ablikim,¹ M. N. Achasov,^{4,b} P. Adlarson,⁷⁵ X. C. Ai,⁸⁰ R. Aliberti,³⁵ A. Amoroso,^{74a,74c} M. R. An,³⁹ Q. An,^{71,58} Y. Bai,⁵⁷ O. Bakina,³⁶ I. Balossino,^{29a} Y. Ban,^{46,g} H.-R. Bao,⁶³ V. Batozskaya,^{1,44} K. Begzsuren,³² N. Berger,³⁵ M. Berlowski,⁴⁴ M. Bertani,^{28a} D. Bettoni,^{29a} F. Bianchi,^{74a,74c} E. Bianco,^{74a,74c} A. Bortone,^{74a,74c} I. Boyko,³⁶ R. A. Briere,⁵ A. Brueggemann,⁶⁸ H. Cai,⁷⁶ X. Cai,^{1,58} A. Calcaterra,^{28a} G. F. Cao,^{1,63} N. Cao,^{1,63} S. A. Cetin,^{62a} J. F. Chang,^{1,58} W. L. Chang,^{1,63} G. R. Che,⁴³ G. Chelkov,^{36,a} C. Chen,⁴³ Chao Chen,⁵⁵ G. Chen,¹ H. S. Chen,^{1,63} M. L. Chen,^{1,58,63} S. J. Chen,⁴² S. L. Chen,⁴⁵ S. M. Chen,⁶¹ T. Chen,^{1,63} X. R. Chen,^{31,63} X. T. Chen,^{1,63} Y. B. Chen,^{1,58} Y. Q. Chen,³⁴ Z. J. Chen,^{25,h} S. K. Choi,¹⁰ X. Chu,⁴³ G. Cibinetto,^{29a} S. C. Coen,³ F. Cossio,^{74c} J. J. Cui,⁵⁰ H. L. Dai,^{1,58} J. P. Dai,⁷⁸ A. Dbeysy,¹⁸ R. E. de Boer,³ D. Dedovich,³⁶ Z. Y. Deng,¹ A. Denig,³⁵ I. Denysenko,³⁶ M. Destefanis,^{74a,74c} F. De Mori,^{74a,74c} B. Ding,^{66,1} X. X. Ding,^{46,g} Y. Ding,³⁴ Y. Ding,⁴⁰ J. Dong,^{1,58} L. Y. Dong,^{1,63} M. Y. Dong,^{1,58,63} X. Dong,⁷⁶ M. C. Du,¹ S. X. Du,⁸⁰ Z. H. Duan,⁴² P. Egorov,^{36,a} Y. H. Fan,⁴⁵ J. Fang,^{1,58} S. S. Fang,^{1,63} W. X. Fang,¹ Y. Fang,¹ Y. Q. Fang,^{1,58} R. Farinelli,^{29a} L. Fava,^{74b,74c} F. Feldbauer,³ G. Felici,^{28a} C. Q. Feng,^{71,58} J. H. Feng,⁵⁹ Y. T. Feng,^{71,58} K. Fischer,⁶⁹ M. Fritsch,³ C. D. Fu,¹ J. L. Fu,⁶³ Y. W. Fu,¹ H. Gao,⁶³ Y. N. Gao,^{46,g} Yang Gao,^{71,58} S. Garbolino,^{74c} I. Garzia,^{29a,29b} P. T. Ge,⁷⁶ Z. W. Ge,⁴² C. Geng,⁵⁹ E. M. Gersabeck,⁶⁷ A. Gilman,⁶⁹ K. Goetzen,¹³ L. Gong,⁴⁰ W. X. Gong,^{1,58} W. Gradl,³⁵ S. Gramigna,^{29a,29b} M. Greco,^{74a,74c} M. H. Gu,^{1,58} Y. T. Gu,¹⁵ C. Y. Guan,^{1,63} Z. L. Guan,²² A. Q. Guo,^{31,63} L. B. Guo,⁴¹ M. J. Guo,⁵⁰ R. P. Guo,⁴⁹ Y. P. Guo,^{12,f} A. Guskov,^{36,a} J. Gutierrez,²⁷ K. L. Han,⁶³ T. T. Han,¹ W. Y. Han,³⁹ X. Q. Hao,¹⁹ F. A. Harris,⁶⁵ K. K. He,⁵⁵ K. L. He,^{1,63} F. H. H. Heinsius,³ C. H. Heinz,³⁵ Y. K. Heng,^{1,58,63} C. Herold,⁶⁰ T. Holtmann,³ P. C. Hong,^{12,f} G. Y. Hou,^{1,63} X. T. Hou,^{1,63} Y. R. Hou,⁶³ Z. L. Hou,¹ B. Y. Hu,⁵⁹ H. M. Hu,^{1,63} J. F. Hu,^{56,i} T. Hu,^{1,58,63} Y. Hu,¹ G. S. Huang,^{71,58} K. X. Huang,⁵⁹ L. Q. Huang,^{31,63} X. T. Huang,⁵⁰ Y. P. Huang,¹ T. Hussain,⁷³ N. Hüskén,^{27,35} N. in der Wiesche,⁶⁸ M. Irshad,^{71,58} J. Jackson,²⁷ S. Jaeger,³ S. Janchiv,³² J. H. Jeong,¹⁰ Q. Ji,¹ Q. P. Ji,¹⁹ X. B. Ji,^{1,63} X. L. Ji,^{1,58} Y. Y. Ji,⁵⁰ X. Q. Jia,⁵⁰ Z. K. Jia,^{71,58} H. B. Jiang,⁷⁶ P. C. Jiang,^{46,g} S. S. Jiang,³⁹ T. J. Jiang,¹⁶ X. S. Jiang,^{1,58,63} Y. Jiang,⁶³ J. B. Jiao,⁵⁰ Z. Jiao,²³ S. Jin,⁴² Y. Jin,⁶⁶ M. Q. Jing,^{1,63} X. M. Jing,⁶³ T. Johansson,⁷⁵ X. K.,¹ S. Kabana,³³ N. Kalantar-Nayestanaki,⁶⁴ X. L. Kang,⁹ X. S. Kang,⁴⁰ M. Kavatsyuk,⁶⁴ B. C. Ke,⁸⁰ V. Khachatryan,²⁷ A. Khoukaz,⁶⁸ R. Kiuchi,¹ O. B. Kolcu,^{62a} B. Kopf,³ M. Kuessner,³ A. Kupsc,^{44,75} W. Kühn,³⁷ J. J. Lane,⁶⁷ P. Larin,¹⁸ L. Lavezzi,^{74a,74c} T. T. Lei,^{71,58} Z. H. Lei,^{71,58} H. Leithoff,³⁵ M. Lellmann,³⁵ T. Lenz,³⁵ C. Li,⁴³ C. Li,⁴⁷ C. H. Li,³⁹ Cheng Li,^{71,58} D. M. Li,⁸⁰ F. Li,^{1,58} G. Li,¹ H. Li,^{71,58} H. B. Li,^{1,63} H. J. Li,¹⁹ H. N. Li,^{56,i} Hui Li,⁴³ J. R. Li,⁶¹ J. S. Li,⁵⁹ J. W. Li,⁵⁰ Ke Li,¹ L. J. Li,^{1,63} L. K. Li,¹ Lei Li,⁴⁸ M. H. Li,⁴³ P. R. Li,^{38,k} Q. X. Li,⁵⁰ S. X. Li,¹² T. Li,⁵⁰ W. D. Li,^{1,63} W. G. Li,¹ X. H. Li,^{71,58} X. L. Li,⁵⁰ Xiaoyu Li,^{1,63} Y. G. Li,^{46,g} Z. J. Li,⁵⁹ Z. X. Li,¹⁵ C. Liang,⁴² H. Liang,^{71,58} H. Liang,^{1,63} Y. F. Liang,⁵⁴ Y. T. Liang,^{31,63} G. R. Liao,¹⁴ L. Z. Liao,⁵⁰ Y. P. Liao,^{1,63} J. Libby,²⁶ A. Limphirat,⁶⁰ D. X. Lin,^{31,63} T. Lin,¹ B. J. Liu,¹ B. X. Liu,⁷⁶ C. Liu,³⁴ C. X. Liu,¹ F. H. Liu,⁵³ Fang Liu,¹ Feng Liu,⁶ G. M. Liu,^{56,i} H. Liu,^{38,j,k} H. B. Liu,¹⁵ H. M. Liu,^{1,63} Huanhuan Liu,¹ Huihui Liu,²¹ J. B. Liu,^{71,58} J. Y. Liu,^{1,63} K. Liu,^{38,j,k} K. Y. Liu,⁴⁰ Ke Liu,²² L. Liu,^{71,58} L. C. Liu,⁴³ Lu Liu,⁴³ M. H. Liu,^{12,f} P. L. Liu,¹ Q. Liu,⁶³ S. B. Liu,^{71,58} T. Liu,^{12,f} W. K. Liu,⁴³ W. M. Liu,^{71,58} X. Liu,^{38,j,k} Y. Liu,^{38,j,k} Y. Liu,⁸⁰ Y. B. Liu,⁴³ Z. A. Liu,^{1,58,63} Z. Q. Liu,⁵⁰ X. C. Lou,^{1,58,63} F. X. Lu,⁵⁹ H. J. Lu,²³ J. G. Lu,^{1,58} X. L. Lu,¹ Y. Lu,⁷ Y. P. Lu,^{1,58} Z. H. Lu,^{1,63} C. L. Luo,⁴¹ M. X. Luo,⁷⁹ T. Luo,^{12,f} X. L. Luo,^{1,58} X. R. Lyu,⁶³ Y. F. Lyu,⁴³ F. C. Ma,⁴⁰ H. Ma,⁷⁸ H. L. Ma,¹ J. L. Ma,^{1,63} L. L. Ma,⁵⁰ M. M. Ma,^{1,63} Q. M. Ma,¹ R. Q. Ma,^{1,63} X. Y. Ma,^{1,58} Y. Ma,^{46,g} Y. M. Ma,³¹ F. E. Maas,¹⁸ M. Maggiora,^{74a,74c} S. Malde,⁶⁹ A. Mangoni,^{28b} Y. J. Mao,^{46,g} Z. P. Mao,¹ S. Marcello,^{74a,74c} Z. X. Meng,⁶⁶ J. G. Messchendorp,^{13,64} G. Mezzadri,^{29a} H. Miao,^{1,63} T. J. Min,⁴² R. E. Mitchell,²⁷ X. H. Mo,^{1,58,63} B. Moses,²⁷ N. Yu. Muchnoi,^{4,b} J. Muskalla,³⁵ Y. Nefedov,³⁶ F. Nerling,^{18,d} I. B. Nikolaev,^{4,b} Z. Ning,^{1,58} S. Nisar,^{11,1} Q. L. Niu,^{38,j,k} W. D. Niu,⁵⁵ Y. Niu,⁵⁰ S. L. Olsen,⁶³ Q. Ouyang,^{1,58,63} S. Pacetti,^{28b,28c} X. Pan,⁵⁵ Y. Pan,⁵⁷ A. Pathak,³⁴ P. Patteri,^{28a} Y. P. Pei,^{71,58} M. Pelizaeus,³ H. P. Peng,^{71,58} Y. Y. Peng,^{38,j,k} K. Peters,^{13,d} J. L. Ping,⁴¹ R. G. Ping,^{1,63} S. Plura,³⁵ V. Prasad,³³ F. Z. Qi,¹ H. Qi,^{71,58} H. R. Qi,⁶¹ M. Qi,⁴² T. Y. Qi,^{12,f} S. Qian,^{1,58} W. B. Qian,⁶³ C. F. Qiao,⁶³ J. J. Qin,⁷² L. Q. Qin,¹⁴ X. S. Qin,⁵⁰ Z. H. Qin,^{1,58} J. F. Qiu,¹ S. Q. Qu,⁶¹ C. F. Redmer,³⁵ K. J. Ren,³⁹ A. Rivetti,^{74c} M. Rolo,^{74c} G. Rong,^{1,63} Ch. Rosner,¹⁸ S. N. Ruan,⁴³ N. Salone,⁴⁴ A. Sarantsev,^{36,c} Y. Schelhaas,³⁵ K. Schoenning,⁷⁵ M. Scodreggio,^{29a,29b} K. Y. Shan,^{12,f} W. Shan,²⁴ X. Y. Shan,^{71,58} J. F. Shangguan,⁵⁵ L. G. Shao,^{1,63} M. Shao,^{71,58} C. P. Shen,^{12,f} H. F. Shen,^{1,63} W. H. Shen,⁶³ X. Y. Shen,^{1,63} B. A. Shi,⁶³ H. C. Shi,^{71,58} J. L. Shi,¹² J. Y. Shi,¹ Q. Q. Shi,⁵⁵ R. S. Shi,^{1,63} X. Shi,^{1,58} J. J. Song,¹⁹ T. Z. Song,⁵⁹ W. M. Song,^{34,1} Y. J. Song,¹² S. Sosio,^{74a,74c} S. Spataro,^{74a,74c} F. Stieler,³⁵ Y. J. Su,⁶³ G. B. Sun,⁷⁶ G. X. Sun,¹ H. Sun,⁶³ H. K. Sun,¹ J. F. Sun,¹⁹ K. Sun,⁶¹ L. Sun,⁷⁶ S. S. Sun,^{1,63} T. Sun,^{51,e} W. Y. Sun,³⁴ Y. Sun,⁹ Y. J. Sun,^{71,58} Y. Z. Sun,¹ Z. T. Sun,⁵⁰ Y. X. Tan,^{71,58} C. J. Tang,⁵⁴ G. Y. Tang,¹ J. Tang,⁵⁹ Y. A. Tang,⁷⁶ L. Y. Tao,⁷² Q. T. Tao,^{25,h} M. Tat,⁶⁹ J. X. Teng,^{71,58} V. Thoren,⁷⁵ W. H. Tian,⁵² W. H. Tian,⁵⁹ Y. Tian,^{31,63} Z. F. Tian,⁷⁶ I. Uman,^{62b} Y. Wan,⁵⁵ S. J. Wang,⁵⁰ B. Wang,¹ B. L. Wang,⁶³ Bo Wang,^{71,58} C. W. Wang,⁴² D. Y. Wang,^{46,g} F. Wang,⁷² H. J. Wang,^{38,j,k} J. P. Wang,⁵⁰ K. Wang,^{1,58} L. L. Wang,¹ M. Wang,⁵⁰ Meng Wang,^{1,63}

N. Y. Wang,⁶³ S. Wang,^{12,f} S. Wang,^{38,j,k} T. Wang,^{12,f} T. J. Wang,⁴³ W. Wang,⁵⁹ W. Wang,⁷² W. P. Wang,^{71,58} X. Wang,^{46,g} X. F. Wang,^{38,j,k} X. J. Wang,³⁹ X. L. Wang,^{12,f} Y. Wang,⁶¹ Y. D. Wang,⁴⁵ Y. F. Wang,^{1,58,63} Y. L. Wang,¹⁹ Y. N. Wang,⁴⁵ Y. Q. Wang,¹ Yaqian Wang,^{17,1} Yi Wang,⁶¹ Z. Wang,^{1,58} Z. L. Wang,⁷² Z. Y. Wang,^{1,63} Ziyi Wang,⁶³ D. Wei,⁷⁰ D. H. Wei,¹⁴ F. Weidner,⁶⁸ S. P. Wen,¹ C. W. Wenzel,³ U. Wiedner,³ G. Wilkinson,⁶⁹ M. Wolke,⁷⁵ L. Wollenberg,³ C. Wu,³⁹ J. F. Wu,^{1,8} L. H. Wu,¹ L. J. Wu,^{1,63} X. Wu,^{12,f} X. H. Wu,³⁴ Y. Wu,⁷¹ Y. H. Wu,⁵⁵ Y. J. Wu,³¹ Z. Wu,^{1,58} L. Xia,^{71,58} X. M. Xian,³⁹ T. Xiang,^{46,g} D. Xiao,^{38,j,k} G. Y. Xiao,⁴² S. Y. Xiao,¹ Y. L. Xiao,^{12,f} Z. J. Xiao,⁴¹ C. Xie,⁴² X. H. Xie,^{46,g} Y. Xie,⁵⁰ Y. G. Xie,^{1,58} Y. H. Xie,⁶ Z. P. Xie,^{71,58} T. Y. Xing,^{1,63} C. F. Xu,^{1,63} C. J. Xu,⁵⁹ G. F. Xu,¹ H. Y. Xu,⁶⁶ Q. J. Xu,¹⁶ Q. N. Xu,³⁰ W. Xu,¹ W. L. Xu,⁶⁶ X. P. Xu,⁵⁵ Y. C. Xu,⁷⁷ Z. P. Xu,⁴² Z. S. Xu,⁶³ F. Yan,^{12,f} L. Yan,^{12,f} W. B. Yan,^{71,58} W. C. Yan,⁸⁰ X. Q. Yan,¹ H. J. Yang,^{51,e} H. L. Yang,³⁴ H. X. Yang,¹ Tao Yang,¹ Y. Yang,^{12,f} Y. F. Yang,⁴³ Y. X. Yang,^{1,63} Yifan Yang,^{1,63} Z. W. Yang,^{38,j,k} Z. P. Yao,⁵⁰ M. Ye,^{1,58} M. H. Ye,⁸ J. H. Yin,¹ Z. Y. You,⁵⁹ B. X. Yu,^{1,58,63} C. X. Yu,⁴³ G. Yu,^{1,63} J. S. Yu,^{25,h} T. Yu,⁷² X. D. Yu,^{46,g} C. Z. Yuan,^{1,63} L. Yuan,² S. C. Yuan,¹ Y. Yuan,^{1,63} Z. Y. Yuan,⁵⁹ C. X. Yue,³⁹ A. A. Zafar,⁷³ F. R. Zeng,⁵⁰ S. H. Zeng,⁷² X. Zeng,^{12,f} Y. Zeng,^{25,h} Y. J. Zeng,^{1,63} X. Y. Zhai,³⁴ Y. C. Zhai,⁵⁰ Y. H. Zhan,⁵⁹ A. Q. Zhang,^{1,63} B. L. Zhang,^{1,63} B. X. Zhang,¹ D. H. Zhang,⁴³ G. Y. Zhang,¹⁹ H. Zhang,⁷¹ H. C. Zhang,^{1,58,63} H. H. Zhang,⁵⁹ H. H. Zhang,³⁴ H. Q. Zhang,^{1,58,63} H. Y. Zhang,^{1,58} J. Zhang,⁸⁰ J. Zhang,⁵⁹ J. J. Zhang,⁵² J. L. Zhang,²⁰ J. Q. Zhang,⁴¹ J. W. Zhang,^{1,58,63} J. X. Zhang,^{38,j,k} J. Y. Zhang,¹ J. Z. Zhang,^{1,63} Jianyu Zhang,⁶³ L. M. Zhang,⁶¹ L. Q. Zhang,⁵⁹ Lei Zhang,⁴² P. Zhang,^{1,63} Q. Y. Zhang,^{39,80} Shuihan Zhang,^{1,63} Shulei Zhang,^{25,h} X. D. Zhang,⁴⁵ X. M. Zhang,¹ X. Y. Zhang,⁵⁰ Y. Zhang,⁶⁹ Y. Zhang,⁷² Y. T. Zhang,⁸⁰ Y. H. Zhang,^{1,58} Yan Zhang,^{71,58} Yao Zhang,¹ Z. D. Zhang,¹ Z. H. Zhang,¹ Z. L. Zhang,³⁴ Z. Y. Zhang,⁴³ Z. Y. Zhang,⁷⁶ G. Zhao,¹ J. Y. Zhao,^{1,63} J. Z. Zhao,^{1,58} Lei Zhao,^{71,58} Ling Zhao,¹ M. G. Zhao,⁴³ R. P. Zhao,⁶³ S. J. Zhao,⁸⁰ Y. B. Zhao,^{1,58} Y. X. Zhao,^{31,63} Z. G. Zhao,^{71,58} A. Zhemchugov,^{36,a} B. Zheng,⁷² J. P. Zheng,^{1,58} W. J. Zheng,^{1,63} Y. H. Zheng,⁶³ B. Zhong,⁴¹ X. Zhong,⁵⁹ H. Zhou,⁵⁰ L. P. Zhou,^{1,63} X. Zhou,⁷⁶ X. K. Zhou,⁶ X. R. Zhou,^{71,58} X. Y. Zhou,³⁹ Y. Z. Zhou,^{12,f} J. Zhu,⁴³ K. Zhu,¹ K. J. Zhu,^{1,58,63} L. Zhu,³⁴ L. X. Zhu,⁶³ S. H. Zhu,⁷⁰ S. Q. Zhu,⁴² T. J. Zhu,^{12,f} W. J. Zhu,^{12,f} Y. C. Zhu,^{71,58} Z. A. Zhu,^{1,63} J. H. Zou,¹ and J. Zu^{71,58}

(BESIII Collaboration)[†]

¹Institute of High Energy Physics, Beijing 100049, People's Republic of China

²Beihang University, Beijing 100191, People's Republic of China

³Bochum Ruhr-University, D-44780 Bochum, Germany

⁴Budker Institute of Nuclear Physics SB RAS (BINP), Novosibirsk 630090, Russia

⁵Carnegie Mellon University, Pittsburgh, Pennsylvania 15213, USA

⁶Central China Normal University, Wuhan 430079, People's Republic of China

⁷Central South University, Changsha 410083, People's Republic of China

⁸China Center of Advanced Science and Technology, Beijing 100190, People's Republic of China

⁹China University of Geosciences, Wuhan 430074, People's Republic of China

¹⁰Chung-Ang University, Seoul, 06974, Republic of Korea

¹¹COMSATS University Islamabad, Lahore Campus, Defence Road, Off Raiwind Road, 54000 Lahore, Pakistan

¹²Fudan University, Shanghai 200433, People's Republic of China

¹³GSI Helmholtzcentre for Heavy Ion Research GmbH, D-64291 Darmstadt, Germany

¹⁴Guangxi Normal University, Guilin 541004, People's Republic of China

¹⁵Guangxi University, Nanning 530004, People's Republic of China

¹⁶Hangzhou Normal University, Hangzhou 310036, People's Republic of China

¹⁷Hebei University, Baoding 071002, People's Republic of China

¹⁸Helmholtz Institute Mainz, Staudinger Weg 18, D-55099 Mainz, Germany

¹⁹Henan Normal University, Xinxiang 453007, People's Republic of China

²⁰Henan University, Kaifeng 475004, People's Republic of China

²¹Henan University of Science and Technology, Luoyang 471003, People's Republic of China

²²Henan University of Technology, Zhengzhou 450001, People's Republic of China

²³Huangshan College, Huangshan 245000, People's Republic of China

²⁴Hunan Normal University, Changsha 410081, People's Republic of China

²⁵Hunan University, Changsha 410082, People's Republic of China

²⁶Indian Institute of Technology Madras, Chennai 600036, India

²⁷Indiana University, Bloomington, Indiana 47405, USA

^{28a}INFN Laboratori Nazionali di Frascati, I-00044, Frascati, Italy

^{28b}INFN Sezione di Perugia, I-06100, Perugia, Italy

- ^{28c}University of Perugia, I-06100, Perugia, Italy
- ^{29a}INFN Sezione di Ferrara, I-44122, Ferrara, Italy
- ^{29b}University of Ferrara, I-44122, Ferrara, Italy
- ³⁰Inner Mongolia University, Hohhot 010021, People's Republic of China
- ³¹Institute of Modern Physics, Lanzhou 730000, People's Republic of China
- ³²Institute of Physics and Technology, Peace Avenue 54B, Ulaanbaatar 13330, Mongolia
- ³³Instituto de Alta Investigación, Universidad de Tarapacá, Casilla 7D, Arica 1000000, Chile
- ³⁴Jilin University, Changchun 130012, People's Republic of China
- ³⁵Johannes Gutenberg University of Mainz, Johann-Joachim-Becher-Weg 45, D-55099 Mainz, Germany
- ³⁶Joint Institute for Nuclear Research, 141980 Dubna, Moscow region, Russia
- ³⁷Justus-Liebig-Universitaet Giessen, II. Physikalisches Institut, Heinrich-Buff-Ring 16, D-35392 Giessen, Germany
- ³⁸Lanzhou University, Lanzhou 730000, People's Republic of China
- ³⁹Liaoning Normal University, Dalian 116029, People's Republic of China
- ⁴⁰Liaoning University, Shenyang 110036, People's Republic of China
- ⁴¹Nanjing Normal University, Nanjing 210023, People's Republic of China
- ⁴²Nanjing University, Nanjing 210093, People's Republic of China
- ⁴³Nankai University, Tianjin 300071, People's Republic of China
- ⁴⁴National Centre for Nuclear Research, Warsaw 02-093, Poland
- ⁴⁵North China Electric Power University, Beijing 102206, People's Republic of China
- ⁴⁶Peking University, Beijing 100871, People's Republic of China
- ⁴⁷Qufu Normal University, Qufu 273165, People's Republic of China
- ⁴⁸Renmin University of China, Beijing 100872, People's Republic of China
- ⁴⁹Shandong Normal University, Jinan 250014, People's Republic of China
- ⁵⁰Shandong University, Jinan 250100, People's Republic of China
- ⁵¹Shanghai Jiao Tong University, Shanghai 200240, People's Republic of China
- ⁵²Shanxi Normal University, Linfen 041004, People's Republic of China
- ⁵³Shanxi University, Taiyuan 030006, People's Republic of China
- ⁵⁴Sichuan University, Chengdu 610064, People's Republic of China
- ⁵⁵Soochow University, Suzhou 215006, People's Republic of China
- ⁵⁶South China Normal University, Guangzhou 510006, People's Republic of China
- ⁵⁷Southeast University, Nanjing 211100, People's Republic of China
- ⁵⁸State Key Laboratory of Particle Detection and Electronics, Beijing 100049, Hefei 230026, People's Republic of China
- ⁵⁹Sun Yat-Sen University, Guangzhou 510275, People's Republic of China
- ⁶⁰Suranaree University of Technology, University Avenue 111, Nakhon Ratchasima 30000, Thailand
- ⁶¹Tsinghua University, Beijing 100084, People's Republic of China
- ^{62a}Turkish Accelerator Center Particle Factory Group, Istinye University, 34010, Istanbul, Turkey
- ^{62b}Near East University, Nicosia, North Cyprus, 99138, Mersin 10, Turkey
- ⁶³University of Chinese Academy of Sciences, Beijing 100049, People's Republic of China
- ⁶⁴University of Groningen, NL-9747 AA Groningen, The Netherlands
- ⁶⁵University of Hawaii, Honolulu, Hawaii 96822, USA
- ⁶⁶University of Jinan, Jinan 250022, People's Republic of China
- ⁶⁷University of Manchester, Oxford Road, Manchester, M13 9PL, United Kingdom
- ⁶⁸University of Muenster, Wilhelm-Klemm-Strasse 9, 48149 Muenster, Germany
- ⁶⁹University of Oxford, Keble Road, Oxford OX13RH, United Kingdom
- ⁷⁰University of Science and Technology Liaoning, Anshan 114051, People's Republic of China
- ⁷¹University of Science and Technology of China, Hefei 230026, People's Republic of China
- ⁷²University of South China, Hengyang 421001, People's Republic of China
- ⁷³University of the Punjab, Lahore-54590, Pakistan
- ^{74a}University of Turin and INFN, University of Turin, I-10125, Turin, Italy
- ^{74b}University of Eastern Piedmont, I-15121, Alessandria, Italy
- ^{74c}INFN, I-10125, Turin, Italy
- ⁷⁵Uppsala University, Box 516, SE-75120 Uppsala, Sweden
- ⁷⁶Wuhan University, Wuhan 430072, People's Republic of China
- ⁷⁷Yantai University, Yantai 264005, People's Republic of China
- ⁷⁸Yunnan University, Kunming 650500, People's Republic of China
- ⁷⁹Zhejiang University, Hangzhou 310027, People's Republic of China
- ⁸⁰Zhengzhou University, Zhengzhou 450001, People's Republic of China

[†]Contact author: besiii-publications@ihep.ac.cn

^aAlso at the Moscow Institute of Physics and Technology, Moscow 141700, Russia.

^bAlso at the Novosibirsk State University, Novosibirsk, 630090, Russia.

^cAlso at the NRC “Kurchatov Institute”, PNPI, 188300, Gatchina, Russia.

^dAlso at Goethe University Frankfurt, 60323 Frankfurt am Main, Germany.

^eAlso at Key Laboratory for Particle Physics, Astrophysics and Cosmology, Ministry of Education; Shanghai Key Laboratory for Particle Physics and Cosmology; Institute of Nuclear and Particle Physics, Shanghai 200240, People’s Republic of China.

^fAlso at Key Laboratory of Nuclear Physics and Ion-beam Application (MOE) and Institute of Modern Physics, Fudan University, Shanghai 200443, People’s Republic of China.

^gAlso at State Key Laboratory of Nuclear Physics and Technology, Peking University, Beijing 100871, People’s Republic of China.

^hAlso at School of Physics and Electronics, Hunan University, Changsha 410082, China.

ⁱAlso at Guangdong Provincial Key Laboratory of Nuclear Science, Institute of Quantum Matter, South China Normal University, Guangzhou 510006, China.

^jAlso at MOE Frontiers Science Center for Rare Isotopes, Lanzhou University, Lanzhou 730000, People’s Republic of China.

^kAlso at Lanzhou Center for Theoretical Physics, Lanzhou University, Lanzhou 730000, People’s Republic of China.

^lAlso at the Department of Mathematical Sciences, IBA, Karachi 75270, Pakistan.